CORE
Metadata, citation and similar papers at core.ac.uk
Provided by Elsevier - Publisher Connector

Available online at www.sciencedirect.com
ScienceDirect
Virology 374 (2008) 151–163
VIROLOGY
www.elsevier.com/locate/yviro

The SARS-CoV ferret model in an infection–challenge study

Yong-Kyu Chu [a], Georgia D. Ali [a], Fuli Jia [a], Qianjun Li [a,*], David Kelvin [b,c], Ronald C. Couch [d], Kevin S. Harrod [d], Julie A. Hutt [d], Cheryl Cameron [b,c], Susan R. Weiss [e], Colleen B. Jonsson [a,*]

[a] *Department of Biochemistry and Molecular Biology, Southern Research Institute, Birmingham, AL, USA*
[b] *University Health Network, Toronto, Ontario, Canada*
[c] *University of Toronto, Toronto, Ontario, Canada*
[d] *Lovelace Respiratory Research Institute, Albuquerque, NM, USA*
[e] *Department of Microbiology, University of Pennsylvania, Philadelphia, PA, USA*

Received 19 September 2007; returned to author for revisions 17 October 2007; accepted 16 December 2007
Available online 29 January 2008

Abstract

Phase I human clinical studies involving therapeutics for emerging and biodefense pathogens with low incidence, such as the severe acute respiratory syndrome coronavirus (SARS-CoV), requires at a minimum preclinical evaluation of efficacy in two well-characterized and robust animal models. Thus, a ferret SARS-CoV model was evaluated over a period of 58 days following extensive optimization and characterization of the model in order to validate clinical, histopathological, virological and immunological endpoints. Ferrets that were infected intranasally with 10^3 $TCID_{50}$ SARS-CoV showed higher body temperature (2–6 d.p.i.), sneezing (5–10 d.p.i.), lesions (5–7 d.p.i.) and decreased WBC/lymphocytes (2–5 d.p.i.). SARS-CoV was detected up to 7 d.p.i. in various tissues and excreta, while neutralizing antibody titers rose at 7 d.p.i. and peaked at 14 d.p.i. At 29 d.p.i., one group was challenged with 10^3 $TCID_{50}$ SARS-CoV, and an anamnestic response in neutralizing antibodies was evident with no detectable virus. This study supports the validity of the ferret model for use in evaluating efficacy of potential therapeutics to treat SARS.
© 2007 Elsevier Inc. All rights reserved.

Keywords: SARS-CoV; Ferret; Animal model

Introduction

Severe acute respiratory syndrome (SARS) is caused by the SARS-coronavirus (SARS-CoV), a positive-sense, single-stranded RNA virus (Drosten et al., 2003; Kuiken et al., 2003a; Peiris et al., 2003a). Pulmonary infection with SARS-CoV can occur in all age groups. The average mortality rate is 9.6%; however, among the elderly the rate is 38% to 50% (Chan et al., 2003a,b; Chiu et al., 2003; Donnelly et al., 2003; Tsui et al., 2003). The potential for SARS-CoV outbreaks is still warranted since palm civets (Guan et al., 2003) and bats (Li et al., 2005) have been implicated as possible zoonotic reservoirs for SARS-CoV or closely related SARS-like viruses.

The discovery and evaluation of effective therapeutics for newly emergent clinical diseases such as SARS-CoV require well-defined animal models. Several groups have reported the use of small animal models which may reproduce some features of SARS in humans. These small animal models, particularly mice (Hogan et al., 2004; Roberts et al., 2005a; Wentworth et al., 2004; Yang et al., 2004) and hamsters (Roberts et al., 2006, 2005b), can provide experimental systems for the study of infectivity, immunity and pathogenesis, while serving as a very useful tools for screening of vaccines and antiviral drugs. However, their utility in the study of the clinical progression of disease is limited by the inherent differences between small mammals and humans in anatomical structure, respiratory physiology and manifestation of clinical disease. Furthermore, FDA approval of vaccines and therapeutics for the treatment of emerging diseases such as SARS requires demonstration of

* Corresponding authors. C.B. Jonsson is to be contacted at Emerging Infectious Disease Research Program, Department of Biochemistry and Molecular Biology, 2000 9th Avenue South, Southern Research Institute, Birmingham, AL 35205, USA. Fax: +34 205 581 2093. Q. Li, Department of Biochemistry and Molecular Biology, Southern Research Institute, Birmingham, AL, USA.
E-mail address: Jonsson@sri.org (C.B. Jonsson).

0042-6822/$ - see front matter © 2007 Elsevier Inc. All rights reserved.
doi:10.1016/j.virol.2007.12.032

efficacy in at least two animal models—a rodent and a nonrodent. The nonhuman primate has been used as a model for studies of clinical progression and evaluation of treatments for SARS-CoV infection and disease pathogenesis. However, there has been animal-to-animal variability in the level of viral replication in the lung tissues from SARS-CoV infected African green monkeys (McAuliffe et al., 2004), cynomolgus macaques (Haagmans and Osterhaus, 2006; Kuiken et al., 2003b; Lawler et al., 2006; Osterhaus et al., 2004) and rhesus macaques (Qin et al., 2005; Rowe et al., 2004; Tang et al., 2005; Zhou et al., 2005). Reported symptoms in SARS-CoV infected cynomolgus macaques (Haagmans and Osterhaus, 2006; Kuiken et al., 2003b; Lawler et al., 2006; Rowe et al., 2004) or rhesus macaque (Li et al., 2005; Qin et al., 2005) included lethargy, skin rash, respiratory distress, interstitial pneumonia, and diffuse alveoli damage. Although nonhuman primate models mimic infection and disease symptoms seen in humans, they are very expensive and require special housing and husbandry practices not available in most BSL3 facilities.

One alternative nonrodent model is the domestic ferret, *Mustela putorius furo*. Ferrets have not been commonly used as animal models; therefore, and the literature sources about them are limited. However, these animals have shown great promise in reproducing human correlates of disease for influenza. Preliminary studies showed that the domestic ferret presents disease symptoms and pathology similar to that observed with SARS-CoV infected humans (Martina et al., 2003). When both cats and ferrets infected with SARS-CoV via the intratracheal route using high-virus titer (up to 10^6 $TCID_{50}$ U/mL), the cats showed no clinical symptoms except shedding virus, whereas the ferrets showed classical symptoms of SARS, including death in some cases, in addition to shedding virus (Martina et al., 2003). These studies suggested that the ferret could be developed into a model for preclinical evaluation of efficacy for SARS-CoV therapeutics.

The overall objective of our efforts was to develop and characterize the ferret model for permissive SARS-CoV infection and disease following intensive optimization of the dosing and various endpoints. Herein, we report the validation of the model in an infection and challenge over 58 days. The study validated standard health indicator endpoints that allow comparisons to clinical manifestation of SARS-CoV in human patients. These included: clinical findings, temperature, mean body weight, hematology and clinical chemistry parameters, gross pathology and histopathology, and virological and immunological assessments. This model will provide insight into understanding many of the underlying features of SARS disease in humans and promote the evaluation of promising therapeutics and vaccines.

Results

Study design

Ferrets were divided randomly into four groups, mock-infected, SARS-CoV infected, mock-challenged, and SARS-CoV challenged (Table 1). The dose of SARS-CoV chosen for these studies was based upon several smaller studies in ferrets with different challenge doses ranging from 10^3 to 10^7 $TCID_{50}$/mL (Fig. 1). In general, the lower dose of virus produced more reproducible results. The lower dose of virus showed less variation in the level of viral infection in the lung. Specifically, the higher dose, 10^7 $TCID_{50}$/mL, showed minimal infection of the ferret nasal turbinates (NT) and variability in the lung. The 10^3 $TCID_{50}$/mL dose provided the highest infection and reproducibility in NT and lung tissues (Fig. 1).

On 0 d.p.i., ferrets in the mock-infected group (Group 1, 18 ferrets) were inoculated intranasally with serum-free medium without virus, and ferrets in the SARS-CoV infected group (Group 2, 42 ferrets) were inoculated intranasally with 10^3 $TCID_{50}$ SARS-CoV diluted in serum-free medium. On 29 d.p.i., nine ferrets from Group 1 were mock-challenged with serum-free medium (Group 3), and eighteen ferrets from Group 2 were challenged with 10^3 TCID50 SARS-CoV (Group 4). Ferrets were observed twice daily, with detailed recording of pharmacological and toxicological signs and symptoms, including nature, onset, severity, and duration of all gross or visible changes (including but not limited to abnormal circulatory, respiratory, excretory, behavioral, and neurological signs and symptoms). In addition, an activity score (0=alert and playful, 1=alert but playful only when stimulated, 2=alert but not playful when stimulated, and 3=neither alert nor playful when stimulated) was obtained each time the ferrets were observed. At predetermined time points, post-inoculation as described in the Materials and Methods, ferrets (three ferrets from Group 1, 3, 4, and four from Group 2) were euthanized, and specimens were collected for analyses of viral load ($TCID_{50}$) and neutralization antibody, viral RNA by RT-PCR, changes in cytology (immunohistochemistry and histopathology) and changes in clinical

Table 1
Study design and key clinical observations

Group	Day 0	Day 29	Number of animals	Sneezing		Diarrhea		Mortality and morbidity
				<day 29	>day 29	<day 29	>day 29	
1 (mock-infected)	SFM	None	18	0/18[a]	None	1/18	None	0/18
2 (SARS-CoV infected)	SARS-CoV (10^3 $TCID_{50}$)	None	42	17/42	None	5/42	None	0/42
3 (mock-challenged)	SFM	SFM	9	None	0/9	None	1/9	0/9
4 (SARS-CoV challenged)	SARS-CoV (10^3 $TCID_{50}$)	SARS-CoV (10^3 $TCID_{50}$)	18	None	0/18	None	5/18	1/18[b]

[a]The indicated clinical observations were expressed as the number of observations/total sample number.
[b]One ferret in this group was euthanized early after developing a moribund state.
SFM: Serum Free media (DMEM).

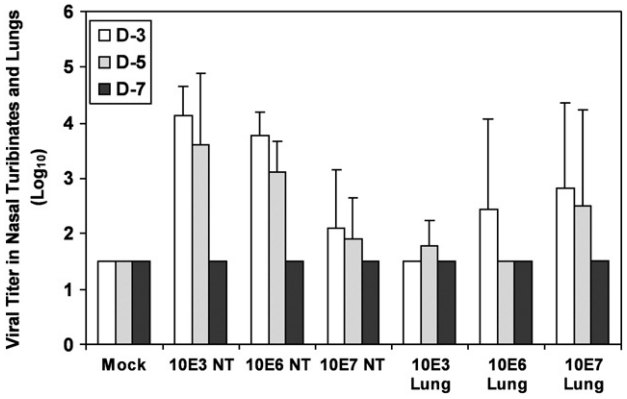

Fig. 1. Titers of SARS-CoV in nasal turbinate (NT) and lung samples from ferrets infected at different doses. Bar graphs show the mean titer of virus detected by $TCID_{50}$ assays on Vero E6 cell monolayer as described in the Materials and Methods. Virus titers are shown for lung and nasal turbinates at three different doses of virus in ferrets: 10^3, 10^5 and 10^7.

pathology (chemistry and hematology) as described in Materials and Methods.

Clinical observations

Subcutaneous body temperatures and clinical observations were obtained twice daily. Graphs of temperature profiles (Fig. 2) depict mean temperatures for the four groups—mock-infected (Group 1), SARS-CoV infected (Group 2), mock-challenged (Group 3) and SARS-CoV challenged (Group 4). Overall, the mean temperatures in all four groups were within the normal range for ferrets, between 35 °C and 39.4 °C, inclusively. Three ferrets in Group 1 had abnormal low body temperature from 1 to 7 d.p.i. In the SARS-CoV infected group (Group 2), temperature increases were evident from 2–7 d.p.i., and statistical analysis showed that there were significant temperature increases on 2 and 6 d.p.i. (*P* value 0.0500 and 0.0157, respectively) as compared to temperatures in mock-infected ferrets (Group 1). Significantly lower temperatures in SARS-CoV infected ferrets were observed on 16 and 24 d.p.i. The interpretation of these findings is unclear. These results support body temperature as a useful marker in assessing SARS-CoV infection in ferrets.

All animals were alert and playful (activity score = 0) with the exception of one ferret in Group 4, which will be discussed later. The clinical observations focused on sneezing, fever, diarrhea, mortality and morbidity (Table 1). While ferrets in the mock-infected Group 1 did not show any sneezing, 17 ferrets among 42 SARS-CoV infected ferrets in Group 2 did. Sneezing was observed as early as 3 d.p.i. and as late as 10 d.p.i. of the study, with most of the sneezing observed between 5 and 10 d.p.i. One ferret among 42 infected ferrets showed both sneezing and ocular discharge, but these two symptoms occurred at different times. No sneezing was observed among 18 SARS-CoV challenged ferrets (Group 4) or the mock-challenged ferrets (Group 3) (Table 1).

Diarrhea was also observed in some ferrets, both in the SARS-CoV infected and mock-infected groups. One ferret in Group 1 had diarrhea at 26 d.p.i., and one ferret in Group 3 showed diarrhea at 15–16 d.p.i. However, five out of 42 ferrets in Group 2 (Table 1) had diarrhea. After challenge, five out of 18 ferrets in Group 4 had diarrhea (Table 1), three showing diarrhea before challenge.

Mortality and morbidity of ferrets were examined twice per day (morning and afternoon) on each day of the study including: identifying dead, weak, or moribund animals; and documenting the onset of any abnormal clinical signs. Moribund animals were defined as those exhibiting: seizures, severe depression, respiratory distress, severe dyspnea (difficult or labored breathing), recumbence and weakness, unresponsiveness to touch and external stimuli, 20% or greater loss in body weight, body temperature below 36.1 °C (indicative of shock), and total anorexia with duration longer than 48 h. Only one ferret from Group 4 had to be euthanized early after developing a moribund state with symptoms including diarrhea, dehydration, hypothermia, and decreased food intake. The disease in this animal was unrelated to SARS-CoV infection as determined by an absence of virus or viral RNA which will be discussed in later sections.

Body weight was taken prior to mock or viral infection/challenge and at necropsy for each group. No significant change

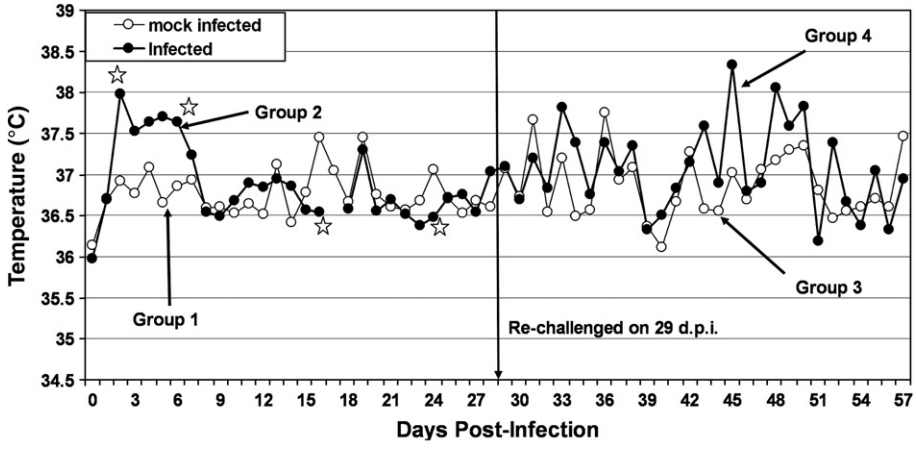

Fig. 2. Daily temperature (°C) fluctuation in mock-infected and SARS-CoV infected ferrets. Significantly higher or lower temperatures are marked with " * ". Group designated and number of animals for each group were indicated in Table 1.

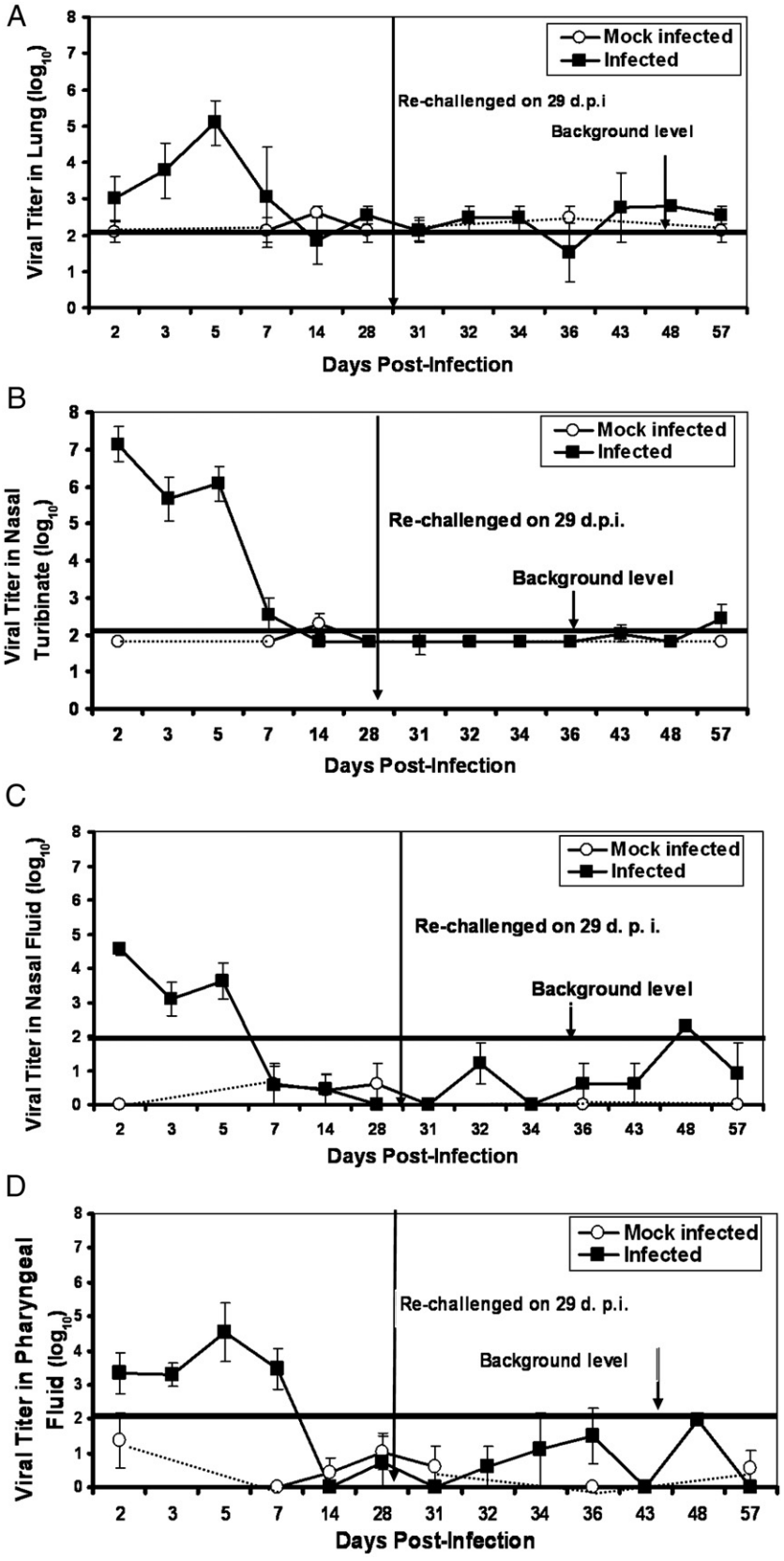

Fig. 3. SARS-CoV titer in different tissues and body fluids collected from mock and SARS-CoV infected ferrets. Line graphs show the mean titer of virus detected by $TCID_{50}$ assays on Vero E6 cell monolayer as described in the Materials and Methods. Virus titers are shown for (A) Lung, (B) Nasal Turbinates, (C) Nasal swabs, and (D) Pharyngeal swabs. Symbols: closed square (virus-infected) and open circle (mock-infected); error bars indicate standard error. Dot line indicates that one or two data points were not available as indicated in the study designed. $n=3$ in Group 1, 3, 4, and $n=4$ in Group 2. Symbols: closed square (virus infected) and open circle (mock-infected).

Table 2
SARS-CoV Toronto 2 vRNA detected in ferret swabs and tissues

SARS-CoV Infected Group 2 (d.p.i.)	NS	PS	RS	T (u)	T (l)	GI (C)	GI (D)	NT	LUNG	LIVER
2	4/4	4/4	0/4	0/4	0/4	0/4	0/4	3/4	2/4	0/4
3	4/4	4/4	0/4	0/4	0/4	0/4	0/4	3/4	1/4	0/4
5	4/4	4/4	1/4	0/4	0/4	0/4	0/4	4/4	4/4	0/4
7	3/4	3/4	0/4	0/4	0/4	0/4	0/4	4/4	4/4	0/4
14	0/4	0/4	0/4	0/4	0/4	0/4	0/4	1/4	0/4	0/4
28	0/4	0/4	0/4	0/4	0/4	0/4	0/4	0/4	0/4	0/4
SARS-CoV Challenged Group 4 (d.p.i.)										
31	0/3	0/3	0/3	0/3	0/3	0/3	0/3	0/3	0/3	0/3
32	0/3	0/3	0/3	0/3	0/3	0/3	0/3	0/3	0/3	0/3
34	0/3	0/3	0/3	0/3	0/3	0/3	0/3	0/3	0/3	0/3
36	0/3	0/3	0/3	0/3	0/3	0/3	0/3	0/3	0/3	0/3
43	0/3	0/3	0/3	0/3	0/3	0/3	0/3	0/3	0/3	0/3
57	0/3	0/3	0/3	0/3	0/3	0/3	0/3	0/3	0/3	0/3

Table shows the number of positive per total sample number analyzed in indicated swab and tissue homogenates. Legend: NS-Nasal Swab; PS-Pharyngeal Swab; RS-Rectal Swab; T(u)-Trachea (upper); T(l) Trachea (lower); GI (C)-GI colon; GI (D)-GI duodenum; NT-Nasal Turbinates.

in mean weight was observed within any group (data not shown). The respective weights for whole lung, liver and heart were obtained at necropsy for all ferrets. A ratio of group mean organ weight to group mean body weight (mean organ wt/mean body wt) was calculated for all groups. The mean lung weight to body weight showed an increase above background in Group 2 ferrets sacrificed on study 7 d.p.i. (data not shown); however, such increases were not statistically significant ($p=0.108$). There were no remarkable differences in mean liver and heart weight (data not shown) between Group 1 and Group 2.

SARS-CoV titer in tissues, nasal, pharyngeal and fecal samples

Viral burdens in the lung, nasal turbinates, upper and lower trachea, duodenum, liver and colon were determined by $TCID_{50}$. Significant viral titers were detected in lung and nasal turbinates tissue from infected animals (Fig. 3). Viral titers in lung tissue were 1 $\log_{10}$ above the background level (10^3 $TCID_{50}$ U/mL) at 2 d.p.i., and increased to 3 $\log_{10}$ above the background level (10^5 $TCID_{50}$ U/mL) at 5 d.p.i. (Fig. 3A). Viral titers in nasal turbinates increased to 5 $\log_{10}$ above background level (10^7 $TCID_{50}$ U/mL) at 2 d.p.i., and decreased slightly at 3 and 5 d.p.i. prior to dropping on day 7 p.i., (10^6 $TCID_{50}$ U/mL) (Fig. 3B). Samples from the liver lysates had high background noise levels, which made the measurement of viral titers difficult. However, virus titers in liver samples were below background levels (data not shown). Similarly, the duodenum, upper trachea and lower trachea had no detectable virus titers (data not shown).

Virus shedding was measured in nasal, pharyngeal and rectal samples. Significant viral titers were detected in nasal and pharyngeal fluids of infected animals (Figs. 3C, D) with 1 to 4 logs above the background level (10^3 to 10^6 $TCID_{50}$/mL). Of note, viral titers post challenge (29 to 57 d.p.i) were generally near or below background (Figs. 3A–D). This suggests that the virus was unable to re-establish an infection in previously infected animals.

Detection of viral RNA by RT-PCR

Total RNA was isolated from tissue homogenates and fluid and excreta swab samples, and analyzed using primers specific for the SARS-CoV nucleocapsid gene. In Group 2, viral RNA was detected in nasal and pharyngeal swabs, nasal turbinates and lung homogenates in the majority of the ferrets from 2 to 7 d.p.i. (Table 2). Overall, the viral RNA levels correlated with viral $TCID_{50}$ titers for individual animals. The rectal swab on day five from a single ferret was positive for viral RNA and correlated with the $TCID_{50}$ result for this animal. On 14 d.p.i., one ferret remained RT-PCR positive; the virus titer for this animal was below the background level. In Groups 1, 3 and 4, no viral RNA was detected in any of the body fluid or tissue samples (Table 2).

As mentioned previously, one ferret in Group 4 exhibited serious health conditions during the course of the study. This ferret had diarrhea from 34 to 48 d.p.i. of the study. On 48 d.p.i., this ferret exhibited dehydration, hypothermia and decreased food intake and was declared as moribund and euthanized. Neither

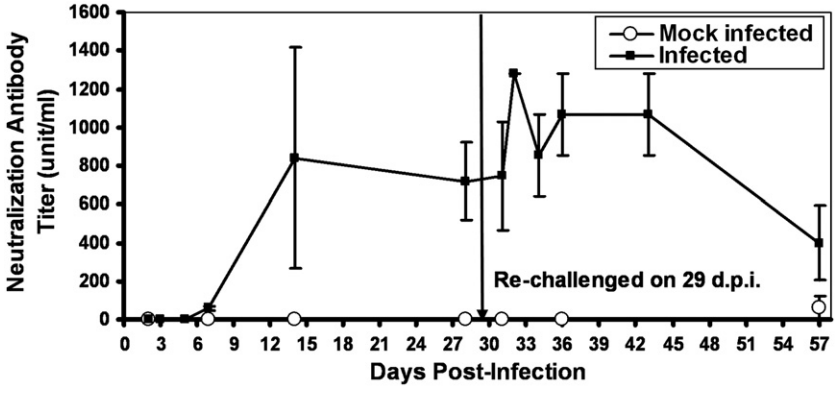

Fig. 4. Reciprocal neutralizing antibody titers from mock or SARS-CoV infected ferrets. Mean antibody titers from three or four ferrets per group are shown. $n=3$ in Group 1, 3, 4, and $n=4$ in Group 2. Symbols: closed square (virus infected) and open circle (mock-infected). Error bars indicate standard errors.

virus nor viral RNA were detected in nasal, colon, duodenum, liver, lung, and lower trachea samples from this ferret; thus, illness was not from SARS-CoV infection.

Neutralization antibody to SARS-CoV

The levels of neutralizing antibody to SARS-CoV were evaluated for all four groups (Fig. 4). No neutralizing antibodies were detected in Groups 1 and 3. In Group 2, neutralizing antibodies increased from 7 d.p.i., reaching a peak titer of 820 U on 14 d.p.i. and decreased slightly to 720 U on 29 d.p.i. before challenge (Fig. 4). The temporal course of neutralizing antibodies correlated with decreasing viral burden in the lung, nasal turbinates, nasal and pharyngeal swab samples at 7 d.p.i. Following SARS-CoV challenge (29 d.p.i.), an anamnestic response was evident for all Group 4 animals with an abrupt increment of neutralizing antibodies to 1300 U, the peak data point for the study. The titers stayed high for about two weeks, and then fell to 400 U by 57 d.p.i.

Histopathology

Sections of lung lobes (left cranial, left caudal, right cranial and right middle), trachea, colon, duodenum, and liver were stained

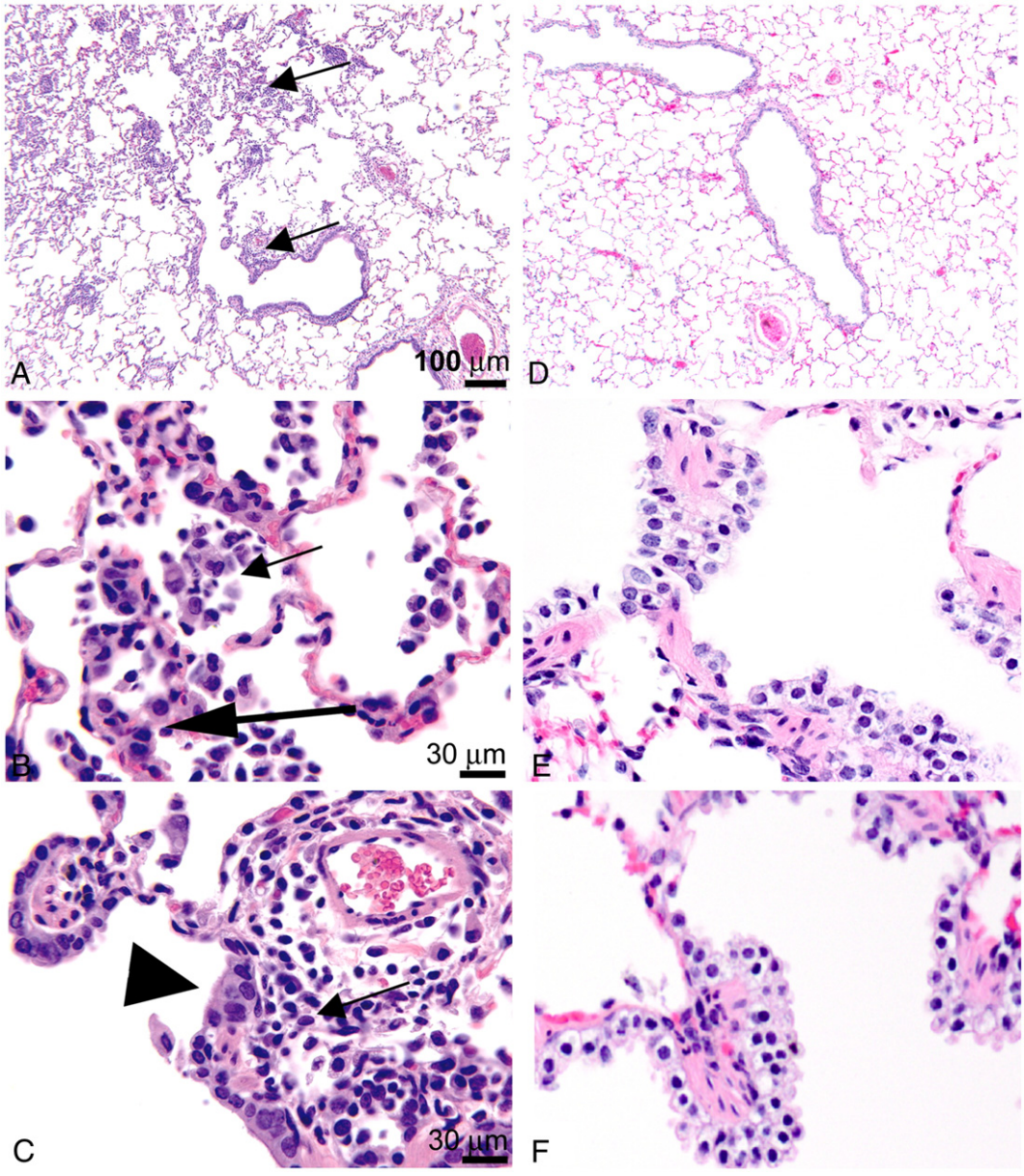

Fig. 5. Representative histologic lesions in lung sections taken on 7 d.p.i. from SARS-CoV (A–C) and mock-infected (D–F) ferrets. (A) Lymphohistiocytic bronchiolar infiltrates with extension into adjacent alveoli (small arrows). (B) Lymphohistiocytic infiltrates in alveolar septae and associated alveoli (small arrow), with type II pneumocyte hyperplasia (large arrow). (C) Lymphohistiocytic infiltrates in the walls of pulmonary vessels and bronchioles (small arrow), with hyperplasia of bronchiolar epithelium (arrowhead). (D) Normal lung from a mock-infected ferret. (E) Normal alveolar septae and alveoli from a mock-infected ferret. (F) Normal bronchoalveolar junction and small blood vessel from a mock-infected ferret.

with hematoxylin and eosin (H&E) staining and evaluated by direct microscopical observation. Lesions were graded subjectively and blindly on a scale of 1 to 4 (1 = minimal, 2 = mild, 3 = moderate, 4 = marked), with distribution modifiers of focal (F), multifocal (M) and diffuse (D).

Lesions related to SARS-CoV infection were identified in the lungs of Group 2 ferrets on 5 and 7 d.p.i. with more severe lesions evident at 7 d.p.i.(Fig. 5A), when compared with the lung lesions from Group 1 animals (Fig. 5D). The primary SARS-related lesion identified in Group 2 animals consisted of lymphohistiocytic bronchointerstitial pneumonia (Fig. 5B). In addition, there was a marked increase in the number of lymphocytes and macrophages associated with the pulmonary vasculature and the connective tissue surrounding conducting airways (Fig. 5C), which was not observed in lungs in Group 1 (Fig. 5F). Severely affected animals developed mild to moderate involvement of bronchi, with luminal accumulation of mucus and neutrophils. A few infected animals also had small collections

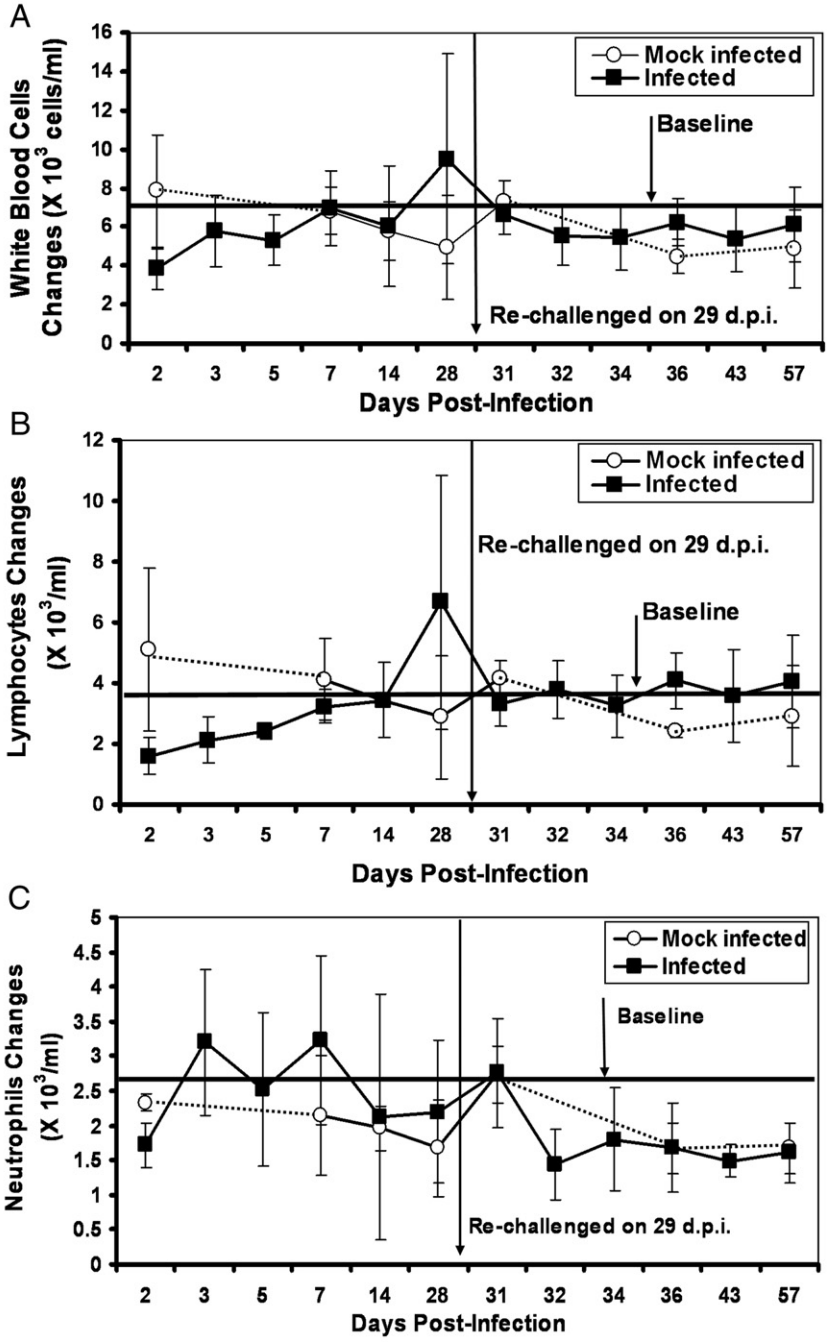

Fig. 6. Clinical hematology of blood samples collected from mock and SARS-CoV infected ferrets. A baseline was obtained from 47 pre-study sera obtained from 26 ferrets. Mock and SARS-CoV infected blood samples were compared with the baseline. Three of the parameters analyzed are presented: (A) White blood cells, (B) Lymphocytes, and (C) Neutrophils. Dot line indicates that one or two data points were not available as indicated in the study designed. $n=3$ in Group 1, 3, 4, and $n=4$ in Group 2. Symbols: closed square (virus infected) and open circle (mock-infected). Error bars indicate standard errors.

of granulocytes (primarily neutrophils) near the bronchioloalveolar junctions. Histologic lesions related to SARS-CoV were not detected among challenged ferrets (results not shown).

Lesions present in many animals from both SARS-CoV exposed and unexposed groups, interpreted to be background lesions unrelated to SARS-CoV exposure, consisted of congestion, minimal to mild peribronchovascular accumulations of lymphocytes, and minimal to mild bronchiolitis.

Clinical chemistry

Baseline values for different clinical chemistry parameters were measured for 60 pre-study serum samples obtained from 30 ferrets. The samples were analyzed for levels of alanine aminotransferase, alkaline phosphatase, albumin, lactate dehydrogenase, aspartate aminotransferase, total bilirubin, blood urea nitrogen, calcium, chloride, cholesterol, creatine kinase, creatinine, gamma glutamyl transferase, glucose, phosphorus, potassium, sodium, total protein, triglyceride, globulin, and albumin/globulin. The group mean values were compared to identify any trends suggestive of SARS-CoV infection. The values from the infected ferrets were compared with the baseline to examine if there was a significant difference. The lactate dehydrogenase levels in serum of Group 2 were significantly higher on 2, 3 and 5 d.p.i. than Group 1 (data not shown) and appear to be a disease marker worthy of further investigation.

Although gamma glutamyl transferase (GGT) was expressed in most of the ferrets, the levels in Group 2 ferrets were generally higher. The baseline value for GGT was negative (very low); hence, it was not included in the comparison. Serum levels of GGT showed some differences between Groups 1 and 2, but they were not significant (results not shown). However, the small sample size ($n=3$ or $n=4$) may have been a factor in the outcome observed in this study; therefore, levels of GGT might warrant further investigation. All other parameters (results not shown), were not significantly different between mock and infected groups (results not shown).

Generally speaking, the major symptom from Group 2 ferrets was dehydration. While dehydration might be a good disease marker, cautions need to be taken to interpret all the clinical chemistry observations.

Hematology

Baseline values for the hematology parameters, including white blood cell count, red blood cell count, hemoglobin concentration, hematocrit, mean corpuscular volume, mean corpuscular hemoglobin, mean corpuscular hemoglobin concentration, neutrophils, lymphocytes, monocytes, eosinophils, basophils, leucocytes, and reticulolocytes were obtained from 47 pre-study blood samples obtained from 26 ferrets. Group 1–4 mean values and the predetermined baseline values (prior to day 0) were plotted on graphs to identify any trends that correlated with SARS-CoV infection (Fig. 6). Values from SARS-CoV infected ferrets (Groups 2 and 4) were compared with mock-infected or challenged (Groups 1 and 3) with the baseline. The levels of white blood cells were significantly lower on 2 d.p.i. (Fig. 6A). Group 2 blood levels of lymphocytes (Fig. 6B) were lower on 2–5 d.p.i and marginally higher on 36 d.p.i. as compared to the baseline value. The level of neutrophils in Group 2 (Fig. 6C) were generally higher than the baseline but were not significant. Group 4 showed levels similar to baseline for all measurements (Figs. 6A–C). All other hematology parameters were not significantly different from the baseline values; however, this may need further confirmation in future experiments using a larger sample size.

Discussion

Patients infected with SARS-CoV show general influenza-like symptoms, fever, headache, malaise, cough, loss of appetite, diarrhea and myalgia (Bitnun et al., 2003; Booth et al., 2003; Chiu et al., 2003; Drosten et al., 2003; Kuiken et al., 2003b; Leung et al., 2003; Peiris et al., 2003b). Older adult patients infected with SARS-CoV often develop a severe febrile pneumonia [for example see (Peiris et al., 2003b)]. In contrast to SARS in adults, SARS in young children tends to be a relatively mild disease. Adolescents can experience significant respiratory disease similar to adults, but younger children generally do not (Bitnun et al., 2003). Symptoms such as myalgias, chills, and headache, which are common in adults, are usually absent in children (Leung et al., 2003; Wong and Fok, 2004). Children have a shorter course of illness, and generally do not develop significant pulmonary disease requiring assisted ventilation (Bitnun et al., 2003; Chiu et al., 2003; Hon et al., 2003; Leung et al., 2003, 2004; Puthucheary et al., 2004). Adults and children appear to have similar levels of SARS-CoV viremia associated with infection, implying that levels of viral replication are similar in both groups (Ng et al., 2003, 2004). Adults with SARS have significantly increased serum levels of inflammatory cytokines and chemokines (Hon et al., 2003; Huang et al., 2005; Wong et al., 2004; Zhang et al., 2004). Activation of inflammatory cytokines in children with SARS may be less dramatic (Ng et al., 2003). Thus, immune response may account for variations in SARS severity between age groups. Development of animal models that reflect these variations in the human population is challenging. However, we noted several parameters common in many of the cases such as temperature, diarrhea, viremia and neutralizing antibody; hence, we sought to discover an animal model that displays these symptoms.

The ferret belongs to the order *Carnivora*, family *Mustelidae*, and is related to mink, otters, and weasels. The domestic (European) ferret (*Mustela putorius furo*) has been domesticated for thousands of years (Ball, 2006). Ferrets have some unique applications including study of human influenza (Renegar, 1992; Smith and Sweet, 1988), and peptic ulcer disease (Del Giudice et al., 2001; Fox et al., 1997). In addition to many basic research applications, ferrets are under active investigation as a nonrodent model in drug development (Fox et al., 1997). More recently, the ferret was explored as a model for SARS; however, the few reports in the literature show apparently conflicting data with regard to infection and pathogenesis of ferret with SARS-CoV, primarily because of differences in study designs, age of animals, and endpoints examined. While Martina et al. have shown that ferrets support SARS-CoV replication and develop pulmonary

lesions (Martina et al., 2003), Weingartl et al. have reported that ferrets remain asymptomatic in the presence of SARS-CoV replication (Weingartl et al., 2004). Herein we have demonstrated that the ferret is a suitable model for permissive SARS-CoV infection, which shows clinically relevant indicators of illness and disease progression. Clinically, we showed temperature increase and sneezing in challenged animals. Fever is one of the disease markers for SARS-CoV infection in humans (Bitnun et al., 2003; Booth et al., 2003; Ksiazek et al., 2003; Kuiken et al., 2003b; Tsui et al., 2003; Wong and Fok, 2004), and in ferrets a temperature increase was significant from 2–6 d.p.i. Sneezing was consistently observed in ferrets from 5–10 d.p.i. (Table 1) but was not observed in mock-infected or challenged ferrets.

In general, the SARS-CoV dose used in the animal models reported to date range from 10^3–10^6 $TCID_{50}$ by intranasal infection. The dose used in this study (10^3) reached similar virus titers used at the higher doses reported. We detected significant levels of SARS-CoV in lung, nasal turbinates, nasal swab and pharyngeal swab samples from infected animals. Virus replication could be detected from 2–7 d.p.i., and the highest peak of virus replication was detected in the upper respiratory region (nasal turbinate) followed by the lower respiratory region (lung). We detected viral RNA by RT-PCR in the nasal and pharyngeal swabs through 7 d.p.i. In general, most animal models show peak days of viral RNA in the lung and nasal turbinate samples from 2 to 7 d.p.i. Ferrets infected with 10^3 or 10^4 $TCID_{50}$, sustain viral replication at 10^6 $TCID_{50}$/mL at 4 d.p.i. (Martina et al., 2003), while ter Meulen et al. show a peak day of infection at 7 d.p.i., in the lung (ter Meulen et al., 2004). Both studies used the SARS-CoV strain HKU-39849. Studies reported by Weingartl et al. and Czub et al., however, showed much longer persistence of viral RNA in lung, pharyngeal and feces samples (Czub et al., 2005; Weingartl et al., 2004). One of the more promising models for SARS-CoV pathogenesis in rodents is the Golden Syrian Hamster, which shows sustained viral replication in the nasal turbinates and lungs (Roberts et al., 2007). After intranasal inoculation with 10^3 $TCID_{50}$ of SARS-CoV, peak viral replication in the lungs occurred at 3 d.p.i. and was cleared by 7 d.p.i; however, viral titers in nasal turbinates were about 10 to 100 folds lower than in lungs and detected through 14 d.p.i.(Roberts et al., 2005b). In our ferret study, viral titers in the nasal turbinates were about 100- to 1000-fold higher (five logs above background) than in the lungs. Virus was also detected in the spleen and liver of the hamster (Roberts et al., 2005b); in contrast, we did not detect virus or viral RNA in the liver of the ferret.

The primary SARS-CoV infection-related lesion in the ferret model was lymphohistiocytic bronchointerstitial pneumonia, which was observed on days 5 and 7 after exposure. In addition, there was a marked increase in the number of lymphocytes and macrophages associated with the pulmonary vasculature and the connective tissue surrounding conducting airways. This kind of pathological presentation has also been observed in SARS-CoV infected nonhuman primates and correlated with the milder syndrome of SARS-CoV infection in human (Kuiken et al., 2004; Lawler et al., 2006; Qin et al., 2005). A relative increase in lung weight, although not significant due to the small sample size, was observed at 7 d.p.i. in infected group, this result corresponded to the period when sneezing was observed.

The occurrence of immune pathology has been a concern in the development of an effective vaccine for SARS (Czub et al., 2005). Disease-enhancing antibodies may be induced after natural viral infections as demonstrated with dengue and feline coronaviruses (Green and Rothman, 2006; Smith and Sweet, 1988; Olsen et al., 1992). Antibodies to the spike protein of the feline coronaviruses are involved in antibody-dependent enhancement of infection. Passive transfer of sera from SARS-CoV infected mice provided protection against subsequent challenge (Subbarao et al., 2004). The absence of histopathological change in the lungs of the challenge group is an indication of the absence of immune pathology in ferrets. The increase in neutralizing antibodies from 7 to 14 d.p.i. correlated with a decrease in viral burden observed in the lung, nasal turbinates, nasal swab and pharyngeal swab samples. Upon challenge one month after primary infection, a significant increase of antibody titers was observed and the antibody titer was higher than that seen after primary infection. The boost in antibody titer may have contributed to the lower viral burden observed after the challenge. Therefore, neutralizing antibodies can be considered as a correlate of protection in SARS-CoV infected animals. In summary, the SARS ferret model and the endpoints identified herein provide a platform for investigations into the immune response and pathogenesis, as well as the evaluation of the efficacy of potential antiviral drugs and vaccines for SARS-CoV disease.

Materials and methods

Virus and cells

SARS-CoV, strain Toronto-2, was provided by Dr. Heinz Feldman at the University of Manitoba. SARS-CoV seed stocks with a titer of 10^7 $TCID_{50}$ U/mL were propagated in Vero E6 cells (ATCC, VERO C1008, CRL 1586). The seed stocks were diluted to the designated titer and used for SARS-CoV $TCID_{50}$ and neutralizing antibody assays.

Ferrets

Male ferrets, *Mustela putorius furo*, 36–45 weeks of age, were purchased from Triple F Farms (Sayre, PA). Ferrets were screened by Triple F Farms for a standard panel of pathogens and at Southern Research Institute for influenza viruses using a standard hemagglutinin assay (Stephenson et al., 2004). Only influenza-free ferrets were used for this study. The pre-study weights of the ferrets ranged from 1 kg to 1.5 kg. The ferrets were uniquely identified by ear tags and subcutaneous transponders (IPTT-300; Biomedic Data Systems Inc, Seaford, Delaware) which were also utilized to measure body temperature. Animal housing and all the animal manipulations were approved by the Animal Care Committee and met the Animal Care guidelines.

SARS-CoV ferret model study design

All animal work was performed in an ABSL3 containment facility. Ferrets were divided randomly into four groups based upon SARS-CoV infection, mock infection, and challenge with

both virus and mock inoculation (Table 1). On 0 d.p.i., twenty-four ferrets (Group 1) were inoculated intranasally with serum-free medium only, and forty-two (Group 2) with SARS-CoV (10^3 $TCID_{50}$/mL) diluted in medium. On 29 d.p.i., nine ferrets (Group 3) were inoculated with serum-free medium, and eighteen ferrets (Group 4) were challenged and inoculated with SARS-CoV (10^3 $TCID_{50}$) diluted in medium. Prior to instillation of mock or virus inoculums, all ferrets were anesthetized, and 1 mL of the inoculum was administered intranasally by drop-wise delivery of 500 μL per nare. Ferrets were observed twice daily, with detailed recording of clinical signs, symptoms, morbidity and mortality including nature, onset, severity, and duration of all gross or visible changes. For the mock-infected group (Groups 1 and 3), three ferrets were sequentially sacrificed on 2, 7, 14, 28, 31, 36, 57 d.p.i (after the first challenge). For SARS-CoV infected (Group 2) and challenged group (Group 4), four (Group 2) and three (Group 4) ferrets were sequentially sacrificed on 2, 3, 5, 7, 14, 28, 31, 32, 34, 36, 43, 57 d.p.i (after the first challenge). Tissue specimens, including lung, nasal turbinates, upper and lower trachea, duodenum, liver and colon; different swab samples, including nasal swab, pharyngeal swab and rectal swab, as well as blood, were collected for various pathological, virological, and immunological tests.

Determination of tissue viral burden

Tissue samples were homogenized to a final 10% (wt/v) suspension in complete DMEM, clarified by low speed centrifugation at 4500 ×*g* for 30 min at 4 °C, and virus titers were determined in Vero E6 cell monolayers grown in 96-well plates. Vero E6 cells were seeded (20,000/well) in a 96-well plate and incubated overnight at 37 °C in a CO_2 incubator. 100 μL of 10-fold serially diluted 10% tissue suspension was added to each well in quadruplicate format. Plates were incubated in a CO_2 incubator at 37 °C for 3 days, after which cytopathic effect (CPE) was observed microscopically at 40× magnification. Virus titers were expressed as $TCID_{50}$ units per gram of tissue, with a lower limit of detection of 10^2 $TCID_{50}$ U/g.

Viral neutralization assay

For the neutralization test, serum samples were two-fold diluted from an initial 1:5 to a final dilution of 1:320, mixed with 60 μL of 2000 $TCID_{50}$/mL of virus and incubated overnight at 4 °C. This was performed in duplicate. The following morning, 100 μL of virus-serum mixture was inoculated to Vero E6 cells which were seeded at 20,000/well as previously prepared. The inoculated plates were incubated in a CO_2 incubator at 37 °C for 3 days, after which CPE of the virus was observed microscopically at 40× magnification.

RNA extraction

Total RNA was extracted from experimental samples, tissue and fluid homogenate suspensions as described for TRIzol LS Reagent (Invitrogen; Carlsbad, CA) according to the manufacturer's instructions. Dried RNA pellets were resuspended in 35 μL of nuclease-free water and stored at −80 °C before RT-PCR amplification was carried out. The RNA was measured for quantity and quality using the Experion Automated Electrophoresis System (Bio-Rad). All RNA extractions were performed in a BSL 2+ Laboratory.

RT-PCR for SARS-CoV

Reverse transcription reactions were performed using Superscript III-Reverse Transcriptase (Invitrogen; Carlsbad, CA) with random primers. Each reaction mixture included 100 ng of random primers, 0.1 to 1.0 μg of total RNA from each sample, and 1 μL of dNTP's (10 mM). The mixture was heated to 65 °C for 5 min and placed on ice for 1 min. The following components were added per reaction: 4 μL 5× first strand buffer; 1 μL DTT (0.1 M); 1 μL RNase OUT; Recombinant RNase Inhibitor; and 1 μL of Superscript III RT (200 U/μL) (Invitrogen). The RT reactions were carried out at 25 °C for 5 min, followed by incubation at 50 °C for 60 min and inactivation of the enzyme at 70 °C for 15 min. To remove RNA in the above mixture, 1 μL of *E. coli* RNase H was added and incubated at 37 °C for another 20 min. All cDNA samples were stored at −20 °C until used for PCR and/or Quantitative Real-Time PCR. For most experimental samples and the positive control (SARS-CoV, Toronto-2 Strain), duplicate cDNA samples were made for each total RNA sample.

Primers from SARS-CoV, Tor-2 strain were used to quantify the amount of viral RNA present in RT samples. The primers are specific for the nucleocapsid (N) gene of the SARS-CoV (GenBank accession # AY274119). The primers sequences used for the PCR detection were as follows: SARS-N-forward 5′-ACC AGA ATG GAG GAC GCA ATG-3′ and SARS-N-reverse 5′-GCT GTG AAC CAA GAC GCA GTA TTA T-3′ (Applied Biosystems; Foster City, CA). A 2–5 μL of each cDNA sample was amplified in a 50 μL reaction that contained 5 μL of 10× High Fidelity PCR Buffer (Invitrogen), 1 μL of each of the 10 μM forward and reverse primers, final 1.5 mM of $MgSO_4$ (50 mM), final 0.2 mM of the dNTP (10 mM) and 2 Units of the HI Fidelity Taq Polymerase (5 U/μL). PCR optimized reactions were incubated at 94 °C for 2 min followed by 30 cycles at 94 °C for 30 s, 56 °C for 30 s, and 68 °C for 30 s and maintained at final 4 °C. All reactions were set up in thin shell 0.2 mL PCR tubes and all reactions were run on a MJ Research Thermal Cycler (Bio-Rad). The PCR products were electrophoresed in a 4% NuSieve agarose gel (Invitrogen).

Clinical chemistry

At necropsy, 1.5 mL whole blood was collected into plastic Gold-top BD Vacutainer SST® Gel tubes with Hemogard™ Closure (3.5 mL draw; BD, Franklin Lakes, NJ). Blood was allowed to clot and then centrifuged for a minimum of 10 min at 1300 ×*g*. Serum was held at 4 to 8 °C until analyzed. Serum samples from all ferrets were analyzed using the Hitachi 911Chemistry Analyzer. Following the manufacturer's manual, the samples were analyzed for levels of alanine aminotransferase, alkaline phosphatase, albumin, lactate dehydrogenase, aspartate aminotransferase, bilirubin-total, blood urea nitrogen, calcium, chloride, cholesterol, creatine kinase, creatinine, gamma glutamyl

transferase, glucose, phosphorus, potassium, sodium, total protein, triglyceride, globulin, and albumin/globulin. Baseline values for these parameters were obtained from 60 pre-study serum samples obtained from 30 ferrets.

Clinical hematology

At necropsy, 1.0 mL whole blood was collected into plastic Lavender-top BD Vacutainer® tubes with Hemogard™ Closure (2 mL draw; BD, Franklin Lakes, NJ) containing EDTA as the anti-coagulant. Whole blood samples were kept at room temperature until analyzed. Blood samples from all ferrets were analyzed using Advia (white blood cell count, red blood cell count, hemoglobin concentration, hematocrit, mean corpuscular volume, mean corpuscular hemoglobin, mean corpuscular hemoglobin concentration, neutrophils, lymphocytes, monocytes, eosinophils, basophils, leucocytes, and reticulolocytes). Baseline values for these parameters were obtained from 47 pre-study blood samples obtained from 26 ferrets. Ferrets are an unidentified species on the Advia, and Bayer protocol states that samples were run using dog species selection. Differences in normal erythrocytes between dogs and ferrets lead to many ferret samples being flagged for microcytosis and/or hypochromasia. Dog MCV normal ranges are 58.8–71.2 fL and ferret MCV normal ranges are 46–65 fL. Dog MCHC normal ranges are 31.0–36.2 g/dL and ferret MCHC normal ranges are 29–36 g/dL. However, manual smear reviews also did not suggest substantive erythrocyte anomalies; thus, these flags may be disregarded in this study.

Histopathology

Mock-infected or SARS-CoV infected ferrets were euthanized and the trachea and lungs were removed *en bloc*. The left cranial (LCr), left caudal (LCd), right cranial (RCr), and right middle (RMi) lung lobes were inflated via a tracheal cannula with 4% paraformaldehyde to approximate normal volume. The inflated lungs were then immersed in 4% paraformaldehyde and allowed to fix for a minimum of 48 h. Sections of trachea, liver, duodenum and colon were also fixed in 4% paraformaldehyde for subsequent histopathology. The fixed tissues were then washed in PBS, and processed routinely for paraffin embedding. Tissue sections (5 μm) were stained with hematoxylin and eosin (H&E) to assess histopathological changes in response to SARS-CoV infection. Multiple tissue sections were examined by a veterinary pathologist. Histopathologic changes were assessed for severity [1 (minimal), 2 (mild), 3 (moderate) and 4 (marked)] and distribution (focal, multifocal, diffuse).

Definitions are as follows:

1) *Bronchiolitis*, mixed, histiocytic and granulocytic: Inflammation of bronchioles characterized by accumulation of histiocytes, eosinophils and/or neutrophils in varying proportions in the walls of bronchioles or at the bronchioloalveolar junction.
2) *Bronchitis,* suppurative, with increased mucus and bronchial epithelial hyperplasia: Inflammation of bronchi characterized by transmigration of neutrophils through the bronchial wall, luminal accumulation of neutrophils and mucus, and variable hyperplasia of bronchial epithelium.
3) *Bronchointerstitial pneumonia*, mononuclear, with type II cell hyperplasia: Inflammation of bronchioles and adjacent alveoli, characterized by infiltrates of lymphocytes and macrophages into the bronchiolar and alveolar septal walls and associated alveoli, with occasional apoptotic/necrotic debris. Bronchiolar epithelial cells vary in appearance from hypertrophied/hyperplastic to flattened and attenuated. Inflammation is often associated with mild type II cell hyperplasia, with variable atypia and infrequent binucleated cells.
4) *Perivascular lymphoid aggregates:* Accumulation of lymphocytes and lesser macrophages adjacent to and sometimes cuffing pulmonary blood vessels.
5) *Peribronchial lymphoid hyperplasia:* Accumulation of lymphocytes and lesser macrophages in the bronchial and/or bronchiolar walls and subjacent connective tissues.
6) *Euthanasia artifact:* Foci of poorly stained tissues with loss of differential staining and loss of nuclear and cytoplasmic detail.

Statistical analysis

Numerical data obtained during the conduct of the study were subjected to calculation of group mean and standard deviation. Differences between group means were analyzed by ANOVA test, with appropriate post tests. P value of 0.05 or less was considered statistically significant. Values were means ± SE. The low numbers of ferrets per group ($n=3$ or 4) made statistical calculations not significant in certain instances. In the clinical chemistry and hematology studies, group means were compared to baseline values as indicated in the text.

Acknowledgments

This research was supported by the NIH Contract N01-AI-30063 (P.I. C.B.J). We thank Charles Gagliano for ferret training provided for this study, Dr. Al Bartolucci for statistical analyses, Kate Buckley for careful review of all the data sets, and Richard Watson for performing SARS-CoV assays. We appreciate the discussions with Drs. Judy Hewitt and Fred Cassals in the development of the model and in review of the manuscript.

References

Ball, R.S., 2006. Issues to consider for preparing ferrets as research subjects in the laboratory. ILAR J. 47, 348–357.

Bitnun, A., Allen, U., Heurter, H., King, S.M., Opavsky, M.A., Ford-Jones, E.L., Matlow, A., Kitai, I., Tellier, R., Richardson, S., Manson, D., Babyn, P., Read, S., 2003. Children hospitalized with severe acute respiratory syndrome-related illness in Toronto. Pediatrics 112, e261.

Booth, C.M., Matukas, L.M., Tomlinson, G.A., Rachlis, A.R., Rose, D.B., Dwosh, H.A., Walmsley, S.L., Mazzulli, T., Avendano, M., Derkach, P., Ephtimios, I.E., Kitai, I., Mederski, B.D., Shadowitz, S.B., Gold, W.L., Hawryluck, L.A., Rea, E., Chenkin, J.S., Cescon, D.W., Poutanen, S.M., Detsky, A.S., 2003. Clinical features and short-term outcomes of 144 patients with SARS in the greater Toronto area. JAMA 289, 2801–2809.

Chan, J.W., Ng, C.K., Chan, Y.H., Mok, T.Y., Lee, S., Chu, S.Y., Law, W.L., Lee, M.P., Li, P.C., 2003a. Short term outcome and risk factors for adverse

clinical outcomes in adults with severe acute respiratory syndrome (SARS). Thorax 58, 686–689.

Chan, P.K., Ip, M., Ng, K.C., Rickjason, C.W., Wu, A., Lee, N., Rainer, T.H., Joynt, G.M., Sung, J.J., Tam, J.S., 2003b. Severe acute respiratory syndrome-associated coronavirus infection. Emerg. Infect. Dis. 9, 1453–1454.

Chiu, W.K., Cheung, P.C., Ng, K.L., Ip, P.L., Sugunan, V.K., Luk, D.C., Ma, L.C., Chan, B.H., Lo, K.L., Lai, W.M., 2003. Severe acute respiratory syndrome in children: experience in a regional hospital in Hong Kong. Pediatr. Crit. Care Med. 4, 279–283.

Czub, M., Weingartl, H., Czub, S., He, R., Cao, J., 2005. Evaluation of modified vaccinia virus Ankara based recombinant SARS vaccine in ferrets. Vaccine 23, 2273–2279.

Del Giudice, G., Covacci, A., Telford, J.L., Montecucco, C., Rappuoli, R., 2001. The design of vaccines against *Helicobacter pylori* and their development. Annu. Rev. Immunol. 19, 523–563.

Donnelly, C.A., Ghani, A.C., Leung, G.M., Hedley, A.J., Fraser, C., Riley, S., Abu-Raddad, L.J., Ho, L.M., Thach, T.Q., Chau, P., Chan, K.P., Lam, T.H., Tse, L.Y., Tsang, T., Liu, S.H., Kong, J.H., Lau, E.M., Ferguson, N.M., Anderson, R.M., 2003. Epidemiological determinants of spread of causal agent of severe acute respiratory syndrome in Hong Kong. Lancet 361, 1761–1766.

Drosten, C., Preiser, W., Gunther, S., Schmitz, H., Doerr, H.W., 2003. Severe acute respiratory syndrome: identification of the etiological agent. Trends Mol. Med. 9, 325–327.

Fox, J.G., Dangler, C.A., Sager, W., Borkowski, R., Gliatto, J.M., 1997. *Helicobacter mustelae*-associated gastric adenocarcinoma in ferrets (*Mustela putorius furo*). Vet. Pathol. 34, 225–229.

Green, S., Rothman, A., 2006. Immunopathological mechanisms in dengue and dengue hemorrhagic fever. Curr. Opin. Infect. Dis. 19 (5), 429–436.

Guan, Y., Zheng, B.J., He, Y.Q., Liu, X.L., Zhuang, Z.X., Cheung, C.L., Luo, S.W., Li, P.H., Zhang, L.J., Guan, Y.J., Butt, K.M., Wong, K.L., Chan, K.W., Lim, W., Shortridge, K.F., Yuen, K.Y., Peiris, J.S., Poon, L.L., 2003. Isolation and characterization of viruses related to the SARS coronavirus from animals in southern China. Science 302, 276–278.

Haagmans, B.L., Osterhaus, A.D., 2006. Nonhuman primate models for SARS. PLoS Med. 3, e194.

Hogan, R.J., Gao, G., Rowe, T., Bell, P., Flieder, D., Paragas, J., Kobinger, G.P., Wivel, N.A., Crystal, R.G., Boyer, J., Feldmann, H., Voss, T.G., Wilson, J.M., 2004. Resolution of primary severe acute respiratory syndrome-associated coronavirus infection requires Stat1. J. Virol. 78, 11416–11421.

Hon, K.L., Leung, C.W., Cheng, W.T., Chan, P.K., Chu, W.C., Kwan, Y.W., Li, A.M., Fong, N.C., Ng, P.C., Chiu, M.C., Li, C.K., Tam, J.S., Fok, T.F., 2003. Clinical presentations and outcome of severe acute respiratory syndrome in children. Lancet 361, 1701–1703.

Huang, K.J., Su, I.J., Theron, M., Wu, Y.C., Lai, S.K., Liu, C.C., Lei, H.Y., 2005. An interferon-gamma-related cytokine storm in SARS patients. J. Med. Virol. 75, 185–194.

Ksiazek, T.G., Erdman, D., Goldsmith, C.S., Zaki, S.R., Peret, T., Emery, S., Tong, S., Urbani, C., Comer, J.A., Lim, W., Rollin, P.E., Dowell, S.F., Ling, A.E., Humphrey, C.D., Shieh, W.J., Guarner, J., Paddock, C.D., Rota, P., Fields, B., DeRisi, J., Yang, J.Y., Cox, N., Hughes, J.M., LeDuc, J.W., Bellini, W.J., Anderson, L.J., 2003. A novel coronavirus associated with severe acute respiratory syndrome. N. Engl. J. Med. 348, 1953–1966.

Kuiken, T., Fouchier, R., Rimmelzwaan, G., Osterhaus, A., 2003a. Emerging viral infections in a rapidly changing world. Curr. Opin. Biotechnol. 14, 641–646.

Kuiken, T., Fouchier, R.A., Schutten, M., Rimmelzwaan, G.F., van Amerongen, G., van Riel, D., Laman, J.D., de Jong, T., van Doornum, G., Lim, W., Ling, A.E., Chan, P.K., Tam, J.S., Zambon, M.C., Gopal, R., Drosten, C., van der Werf, S., Escriou, N., Manuguerra, J.C., Stohr, K., Peiris, J.S., Osterhaus, A.D., 2003b. Newly discovered coronavirus as the primary cause of severe acute respiratory syndrome. Lancet 362, 263–270.

Kuiken, T., van den Hoogen, B.G., van Riel, D.A., Laman, J.D., van Amerongen, G., Sprong, L., Fouchier, R.A., Osterhaus, A.D., 2004. Experimental human metapneumovirus infection of cynomolgus macaques (*Macaca fascicularis*) results in virus replication in ciliated epithelial cells and pneumocytes with associated lesions throughout the respiratory tract. Am. J. Pathol. 164, 1893–1900.

Lawler, J.V., Endy, T.P., Hensley, L.E., Garrison, A., Fritz, E.A., Lesar, M., Baric, R.S., Kulesh, D.A., Norwood, D.A., Wasieloski, L.P., Ulrich, M.P., Slezak, T.R., Vitalis, E., Huggins, J.W., Jahrling, P.B., Paragas, J., 2006. Cynomolgus macaque as an animal model for severe acute respiratory syndrome. PLoS Med. 3 (5), e149.

Leung, T.F., Wong, G.W., Hon, K.L., Fok, T.F., 2003. Severe acute respiratory syndrome (SARS) in children: epidemiology, presentation and management. Paediatr. Respir. Rev. 4, 334–339.

Leung, C.W., Kwan, Y.W., Ko, P.W., Chiu, S.S., Loung, P.Y., Fong, N.C., Lee, L.P., Hui, Y.W., Law, H.K., Wong, W.H., Chan, K.H., Peiris, J.S., Lim, W.W., Lau, Y.L., Chiu, M.C., 2004. Severe acute respiratory syndrome among children. Pediatrics 113, e535–e543.

Li, W., Shi, Z., Yu, M., Ren, W., Smith, C., Epstein, J.H., Wang, H., Crameri, G., Hu, Z., Zhang, H., Zhang, J., McEachern, J., Field, H., Daszak, P., Eaton, B.T., Zhang, S., Wang, L.F., 2005. Bats are natural reservoirs of SARS-like coronaviruses. Science 310, 676–679.

Martina, B.E., Haagmans, B.L., Kuiken, T., Fouchier, R.A., Rimmelzwaan, G.F., Van Amerongen, G., Peiris, J.S., Lim, W., Osterhaus, A.D., 2003. Virology: SARS virus infection of cats and ferrets. Nature 425, 915.

McAuliffe, J., Vogel, L., Roberts, A., Fahle, G., Fischer, S., Shieh, W.J., Butler, E., Zaki, S., St Claire, M., Murphy, B., Subbarao, K., 2004. Replication of SARS coronavirus administered into the respiratory tract of African green, rhesus and cynomolgus monkeys. Virology 330, 8–15.

Ng, E.K., Ng, P.C., Hon, K.L., Cheng, W.T., Hung, E.C., Chan, K.C., Chiu, R.W., Li, A.M., Poon, L.L., Hui, D.S., Tam, J.S., Fok, T.F., Lo, Y.M., 2003. Serial analysis of the plasma concentration of SARS coronavirus RNA in pediatric patients with severe acute respiratory syndrome. Clin. Chem. 49, 2085–2088.

Ng, P.C., Lam, C.W., Li, A.M., Wong, C.K., Cheng, F.W., Leung, T.F., Hon, E.K., Chan, I.H., Li, C.K., Fung, K.S., Fok, T.F., 2004. Inflammatory cytokine profile in children with severe acute respiratory syndrome. Pediatrics 113 (1 Pt 1), e7–e14.

Olsen, C.W., Corapi, W.V., Ngichabe, C.K., Baines, J.D., Scott, F.W., 1992. Monoclonal antibodies to the spike protein of feline infectious peritonitis virus mediate antibody-dependent enhancement of infection of feline macrophages. J. Virol. 66, 956–965.

Osterhaus, A.D., Fouchier, R.A., Kuiken, T., 2004. The aetiology of SARS: Koch's postulates fulfilled. Philos. Trans. R. Soc. Lond., B Biol. Sci. 359, 1081–1082.

Peiris, J.S., Lai, S.T., Poon, L.L., Guan, Y., Yam, L.Y., Lim, W., Nicholls, J., Yee, W.K., Yan, W.W., Cheung, M.T., Cheng, V.C., Chan, K.H., Tsang, D.N., Yung, R.W., Ng, T.K., Yuen, K.Y., 2003a. Coronavirus as a possible cause of severe acute respiratory syndrome. Lancet 361, 1319–1325.

Peiris, J.S., Yuen, K.Y., Osterhaus, A.D., Stohr, K., 2003b. The severe acute respiratory syndrome. N. Engl. J. Med. 349, 2431–2441.

Puthucheary, J., Lim, D., Chan, I., Chay, O.M., Choo, P., 2004. Severe acute respiratory syndrome in Singapore. Arch. Dis. Child. 89, 551–556.

Qin, C., Wang, J., Wei, Q., She, M., Marasco, W.A., Jiang, H., Tu, X., Zhu, H., Ren, L., Gao, H., Guo, L., Huang, L., Yang, R., Cong, Z., Wang, Y., Liu, Y., Sun, Y., Duan, S., Qu, J., Chen, L., Tong, W., Ruan, L., Liu, P., Zhang, H., Zhang, J., Liu, D., Liu, Q., Hong, T., He, W., 2005. An animal model of SARS produced by infection of *Macaca mulatta* with SARS coronavirus. J. Pathol. 206, 251–259.

Renegar, K.B., 1992. Influenza virus infections and immunity: a review of human and animal models. Lab. Anim. Sci. 42, 222–232.

Roberts, A., Paddock, C., Vogel, L., Butler, E., Zaki, S., Subbarao, K., 2005a. Aged BALB/c mice as a model for increased severity of severe acute respiratory syndrome in elderly humans. J. Virol. 79, 5833–5838.

Roberts, A., Vogel, L., Guarner, J., Hayes, N., Murphy, B., Zaki, S., Subbarao, K., 2005b. Severe acute respiratory syndrome coronavirus infection of golden Syrian hamsters. J. Virol. 79, 503–511.

Roberts, A., Thomas, W.D., Guarner, J., Lamirande, E.W., Babcock, G.J., Greenough, T.C., Vogel, L., Hayes, N., Sullivan, J.L., Zaki, S., Subbarao, K., Ambrosino, D.M., 2006. Therapy with a severe acute respiratory syndrome-associated coronavirus-neutralizing human monoclonal antibody reduces disease severity and viral burden in golden Syrian hamsters. J. Infect. Dis. 193, 685–692.

Roberts, A., Deming, D., Paddock, C.D., Cheng, A., Yount, B., Vogel, L., Herman, B.D., Sheahan, T., Heise, M., Genrich, G.L., Zaki, S.R., Baric, R., Subbarao, K., 2007. A mouse-adapted SARS-coronavirus causes disease and mortality in BALB/c mice. PLoS Pathog. 3, e5.

Rowe, T., Gao, G., Hogan, R.J., Crystal, R.G., Voss, T.G., Grant, R.L., Bell, P., Kobinger, G.P., Wivel, N.A., Wilson, J.M., 2004. Macaque model for severe acute respiratory syndrome. J. Virol. 78, 11401–11404.

Smith, H., Sweet, C., 1988. Lessons for human influenza from pathogenicity studies with ferrets. Rev. Infect. Dis. 10, 56–75.

Stephenson, I., Wood, J.M., Nicholson, K.G., Charlett, A., Zambon, M.C., 2004. Detection of anti-H5 responses in human sera by HI using horse erythrocytes following MF59-adjuvanted influenza A/Duck/Singapore/97 vaccine. Virus Res. 103 (1–2), 91–95.

Subbarao, K., McAuliffe, J., Vogel, L., Fahle, G., Fischer, S., Tatti, K., Packard, M., Shieh, W.J., Zaki, S., Murphy, B., 2004. Prior infection and passive transfer of neutralizing antibody prevent replication of severe acute respiratory syndrome coronavirus in the respiratory tract of mice. J. Virol. 78 (7), 3572–3577.

Tang, Q., Zhao, X.Q., Wang, H.Y., Simayi, B., Zhang, Y.Z., Saijo, M., Morikawa, S., Liang, G.D., Kurane, I., 2005. Molecular epidemiology of Xinjiang hemorrhagic fever viruses. Zhonghua Shi Yan He Lin Chuang Bing Du Xue Za Zhi 19, 312–318.

ter Meulen, J., Bakker, A.B., van den Brink, E.N., Weverling, G.J., Martina, B.E., Haagmans, B.L., Kuiken, T., de Kruif, J., Preiser, W., Spaan, W., Gelderblom, H.R., Goudsmit, J., Osterhaus, A.D., 2004. Human monoclonal antibody as prophylaxis for SARS coronavirus infection in ferrets. Lancet 363, 2139–2141.

Tsui, P.T., Kwok, M.L., Yuen, H., Lai, S.T., 2003. Severe acute respiratory syndrome: clinical outcome and prognostic correlates. Emerg. Infect. Dis. 9, 1064–1069.

Weingartl, H., Czub, M., Czub, S., Neufeld, J., Marszal, P., Gren, J., Smith, G., Jones, S., Proulx, R., Deschambault, Y., Grudeski, E., Andonov, A., He, R., Li, Y., Copps, J., Grolla, A., Dick, D., Berry, J., Ganske, S., Manning, L., Cao, J., 2004. Immunization with modified vaccinia virus Ankara-based recombinant vaccine against severe acute respiratory syndrome is associated with enhanced hepatitis in ferrets. J. Virol. 78, 12672–12676.

Wentworth, D.E., Gillim-Ross, L., Espina, N., Bernard, K.A., 2004. Mice susceptible to SARS coronavirus. Emerg. Infect. Dis. 10, 1293–1296.

Wong, G.W., Fok, T.F., 2004. Severe acute respiratory syndrome (SARS) in children. Pediatr. Pulmonol., Suppl. 26, 69–71.

Wong, C.K., Lam, C.W., Wu, A.K., Ip, W.K., Lee, N.L., Chan, I.H., Lit, L.C., Hui, D.S., Chan, M.H., Chung, S.S., Sung, J.J., 2004. Plasma inflammatory cytokines and chemokines in severe acute respiratory syndrome. Clin. Exp. Immunol. 136, 95–103.

Yang, Z.Y., Kong, W.P., Huang, Y., Roberts, A., Murphy, B.R., Subbarao, K., Nabel, G.J., 2004. A DNA vaccine induces SARS coronavirus neutralization and protective immunity in mice. Nature 428, 561–564.

Zhang, Y., Li, J., Zhan, Y., Wu, L., Yu, X., Zhang, W., Ye, L., Xu, S., Sun, R., Wang, Y., Lou, J., 2004. Analysis of serum cytokines in patients with severe acute respiratory syndrome. Infect. Immun. 72, 4410–4415.

Zhou, J., Wang, W., Zhong, Q., Hou, W., Yang, Z., Xiao, S.Y., Zhu, R., Tang, Z., Wang, Y., Xian, Q., Tang, H., Wen, L., 2005. Immunogenicity, safety, and protective efficacy of an inactivated SARS-associated coronavirus vaccine in rhesus monkeys. Vaccine 23, 3202–3209.